

Advancements and Challenges in Wire Arc Additive Manufacturing – A Review

Camilla Kong¹, Azfi Zaidi Mohammad Sofi^{1,2,*}, Sarizam Mamat^{1,2}

¹Faculty of Bioengineering and Technology, Universiti Malaysia Kelantan, 17600 Jeli, Kelantan, Malaysia

²Intelligent Manufacturing Technology Research Group, Faculty of Bioengineering and Technology, Universiti Malaysia Kelantan, 17600 Jeli, Kelantan, Malaysia

*Corresponding author: azfi.ms@umk.edu.my

ARTICLE INFO

Received: 10 November 2024
Accepted: 1 December 2024
Online: 18 December 2024
eISSN: 3036-017X

ABSTRACT

Wire arc additive manufacturing (WAAM) is a groundbreaking advancement in 3D metal printing, enabling efficient and cost-effective production of large, complex components using gas tungsten arc welding (GTAW) and gas metal arc welding (GMAW). Suitable for metals like stainless steel, aluminium, and titanium alloys, WAAM involves layer-by-layer deposition of molten metal using an electric arc to melt wire feedstock. Despite its benefits, WAAM faces challenges with thermal cycles and microstructural inconsistencies, affecting component strength and ductility. Recent studies focus on microstructural analysis and mechanical properties, revealing varied microstructures due to distinct heat cycles. Research indicates consistent hardness across WAAM-fabricated components, with variations based on microstructural constituents. Optimizing the WAAM process involves understanding these characteristics and refining welding parameters. Advances in WAAM technology promise significant improvements in manufacturing efficiency, cost-effectiveness, and component quality across various industries.

Keywords: Additive manufacturing; wire arc additive manufacturing; microstructure; mechanical properties

1. Additive Manufacturing

1.1 Introduction to Additive Manufacturing

Additive manufacturing, also known as a 3-Dimensional (3D) printing process, revolutionizes traditional manufacturing by enabling the production of complex geometries through a layer-by-layer approach. Unlike subtractive manufacturing methods, which involve removing material from a solid block, additive manufacturing builds up materials sequentially until the desired final product is formed. This innovative process allows for unparalleled customization of the final product's shape, making it possible to create intricate and previously unachievable designs. Additionally, additive manufacturing significantly reduces material waste. This not only leads to cost savings but also aligns with sustainable practices. Moreover, the flexibility of additive manufacturing enables rapid prototyping, allowing for faster iteration and development of new designs. The technology's ability to produce complex internal structures and lightweight components has vast applications across various industries, driving forward the possibilities of innovative design and manufacturing efficiency [1].

1.2 Workflow of Additive Manufacturing

The workflow of an additive manufacturing process involves several critical stages [2], each contributing to the successful creation of a 3D-printed object. Initially, the process begins with designing, where digital models of the final product are meticulously created using computer-aided design (CAD) software. These digital models must be highly precise, as they form the blueprint for the subsequent stages. Following the design phase, the modelling stage takes place. Here, the digital models are sliced into numerous thin layers, with each layer representing a cross-sectional slice of the final product. This step is crucial as it determines how the material will be deposited layer-by-layer during the printing phase. In the printing stage, the raw materials, which could be polymers, metals, ceramics, or composites, are deposited layer-by-layer in a controlled manner to build up the shape of the final product. This deposition is guided by the digital model's sliced layers, ensuring that the material is added precisely where needed. Advanced printers employ various techniques such as fused deposition modelling, selective laser sintering, or direct energy deposition to achieve the desired outcome. The precision in this stage is paramount, as any deviation can affect the structural integrity and accuracy of the final product. Finally, the post-processing stage encompasses several finishing steps to refine the printed object. These steps can include curing, which solidifies the material, polishing to smooth surfaces, and heat treatment processes to enhance the mechanical properties of the material. Depending on the complexity and intended use of the product, additional post-processing methods such as machining, painting, or coating might be applied. This stage ensures that the final product not only meets design specifications but also adheres to the required quality standards for its intended application.

1.3 Materials and Technologies in Additive Manufacturing

Ponis et al. [3] identified a diverse range of materials and technologies integral to the additive manufacturing process. This innovative process allows for the creation of complex geometries with minimal waste and unparalleled customization. The materials involved include polymers, which are widely used in rapid prototyping, medical devices, and consumer goods due to their versatility. Metals are crucial for tooling, automotive, and aerospace applications, providing strength and durability. Ceramics are essential for aerospace components, electronics, and dental implants due to their high-temperature resistance and hardness. Composites offer unique properties by combining different materials, resulting in lightweight yet strong parts. The technologies that drive additive manufacturing are equally varied. Binder jetting involves selectively bonding layers of powdered materials using a binder, enabling the creation of complex shapes. Direct energy deposition uses a focused energy source to deposit materials precisely, which is suitable for repairing and adding to existing components. Material extrusion, or fused deposition modelling (FDM), involves heating raw materials and extruding them layer-by-layer. Selective laser sintering/melting employs laser technology to fuse powdered metals and polymers into solid forms. VAT polymerization uses UV light to cure liquid resin layer-by-layer, producing highly detailed and smooth-surfaced parts. These advancements in materials and technologies have significantly expanded the capabilities of additive manufacturing. They enable the production of innovative and high-performance parts across various industries, pushing the boundaries of what is possible. As research and development in additive manufacturing continue to progress, the potential for new applications and improvements in efficiency, cost-effectiveness, and quality will grow, solidifying additive manufacturing's role in the future of manufacturing.

2. Wire Arc Additive Manufacturing (WAAM)

2.1 Introduction to WAAM

Wire and arc additive manufacturing (WAAM) is a 3D metal printing technology that holds significant promise for large-scale manufacturing across various industries. Classified as a direct energy deposition (DED) process, WAAM employs electric arc welding to create 3D metal components through a layer-by-layer deposition method [4]. In this process, a metal wire or electrode serves as the feedstock, which is melted by an electric arc and precisely deposited, often with the assistance of robotic arms, to ensure accuracy and consistency [5]. This method allows for the efficient formation of complex shapes with minimal waste. WAAM can work with a broad range of metals, including stainless steels, aluminium alloys, titanium alloys, and nickel-based alloys, making it highly versatile. Despite its benefits, WAAM faces challenges such as thermal cycles and microstructural inconsistencies, which can affect the mechanical

properties of the final components. Recent research has focused on optimizing these processes to enhance the strength and reliability of WAAM-fabricated components, underscoring the technology's potential for revolutionizing manufacturing efficiency and design innovation. Fig 1, extracted from the research journal by McAndrew et al. [6], illustrates how the WAAM process uses an electric arc to deposit molten metal layer by layer, creating complex metal components.

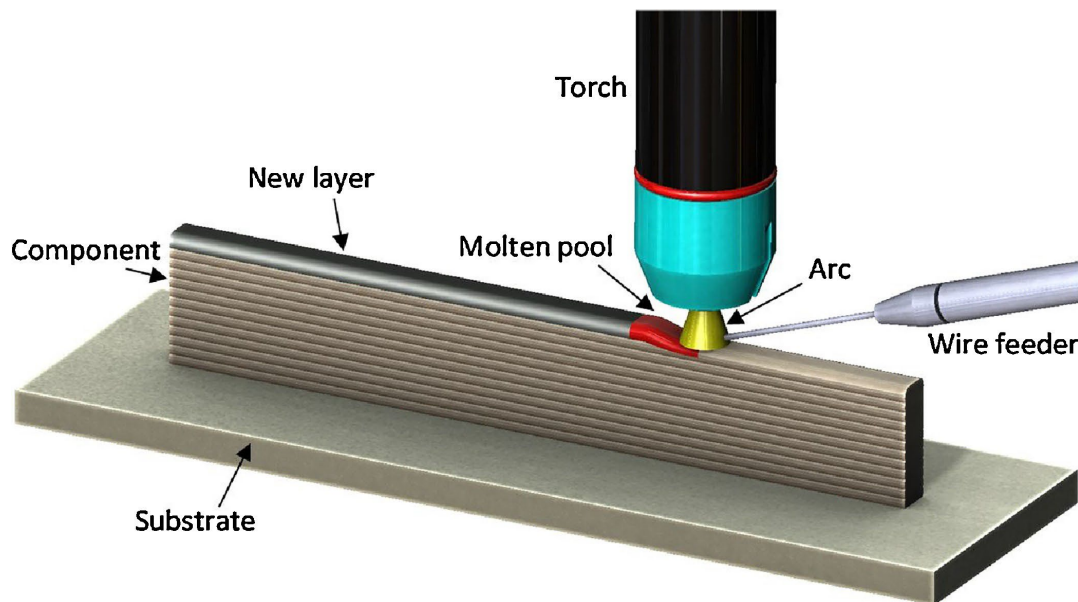


Fig 1: Depiction of the WAAM process extracted from research article by McAndrew et al. [6]

2.2 Benefits of WAAM

In recent years, the wire and arc additive manufacturing (WAAM) process has been gaining significant attention, especially in the manufacturing sectors, due to several key factors [7]. Firstly, WAAM excels at printing large-scale and complex-shaped metal components, a capability that surpasses powder bed fusion (PBF) technologies, which are typically limited to smaller and higher-definition components. Secondly, WAAM is more cost-efficient than PBF technologies. The cost-effectiveness of WAAM stems from the lower cost of welding electrodes compared to the powdered metal used in PBF technologies. Additionally, WAAM often requires only off-the-shelf welding equipment, which is less costly than specialized 3D printers. Lastly, components manufactured using the WAAM process are known for their excellent mechanical properties, often surpassing those of traditionally manufactured components. The use of dense wire feedstock in the WAAM process helps to minimize porosity in the final components, resulting in robust and reliable products [8]. These attributes highlight the growing importance and potential of WAAM in various industrial applications, underscoring its role in advancing manufacturing efficiency and quality.

2.3 Welding Techniques and Challenges in WAAM

Gas tungsten arc welding (GTAW) and gas metal arc welding (GMAW) process are some of the most commonly used welding procedures when it comes to the WAAM manufacturing technology. Several research has been conducted extensively to study the potential of the GMAW-based WAAM process, and these studies have been focused on investigating the technological difficulties and metallurgical properties of various alloy materials. For example, Chen et al. [9] investigated the microstructural formation and tensile strength of 316 L austenitic stainless steel fabricated using the GMAW-based additive manufacturing method. On the other hand, Xiong et al. [10] studied the effect of the welding process parameters on the surface roughness of low-carbon steel products fabricated using the GMAW-based additive manufacturing process. Yang et al. [11] investigated the feasibility of depositing molten steel using a double-electrode GMAW-based additive manufacturing method.

The conventional GMAW method and the wire arc additive manufacturing technologies are common in terms of fabrication perspectives. Hence, the challenges and difficulties that arise associated with both processes may be similar. An example of a disadvantage which may arise is often caused by the thermal cycles during a layer-by-layer deposition strategies of WAAM and can bring a negative impact on the strength and ductility in steel materials, resulting in either the formation of localised brittle zones (LBZs) along the inter-layer regions of multi-layer welding deposition methods [12-13], or the softening of the heat affected zones (HAZs) [14]. Hence, an arc welding technique which can operate with low heat input and high deposition strategy can be beneficial for the applications of the WAAM process.

Challenges which may arise when ferrous alloys are utilized for the WAAM process may depend on the carbon content of the materials, the alloying elements, and the cooling rate of the steel. The said properties of these ferrous alloys can result in the manufactured components having a mixture of different microstructural formations, which can include the formation of ferrite, Widmanstätten ferrite, acicular ferrite, martensite, and bainite [15]. Hence, choosing and determining the proper parameters of the GMAW process is crucial in order to achieve microstructural formation which can contribute to enhanced strength and toughness of final components produced by WAAM.

3. Recent Studies Related to WAAM

3.1 Microstructural Analysis

Liberini et al. [16] conducted research on the deposition of molten weld metal which utilizes the ER70S-6 welding electrode using the GMAW-based additive manufacturing method. In their research, unhomogenized microstructural formation was found throughout the as-built thin wall. Fig 2 depicts the macrography results extracted from their research journal. A bainitic (B) lamellar structure forms in the upper zone (Fig 2c) of the thin wall with equiaxed ferrite (F) grains in the middle zone (Fig 2b) of the thin wall, and a ferritic (F) microstructure with thin pearlite (P) strips at the lower zone (Fig 2a) of the thin wall. Hence, their results concluded that distinct heat cycles caused by the layer-by-layer molten metal deposition characteristic of the WAAM process can result in the formation of a variety of microstructures throughout the final product. The research by Liberini et al. [16] also shows the formation of equiaxed grains with narrow lamellae scattered around the lower zone of the as-built thin wall. The thermal shock occurs when high-temperature molten metal comes in contact with low-temperature base metal, resulting in the formation of ferrite (F) grains and pearlite (P) lamellae. The mild carbon steel used in their research explains the existence of ferrite grains coexisting with thin strips of pearlite microstructure [17].

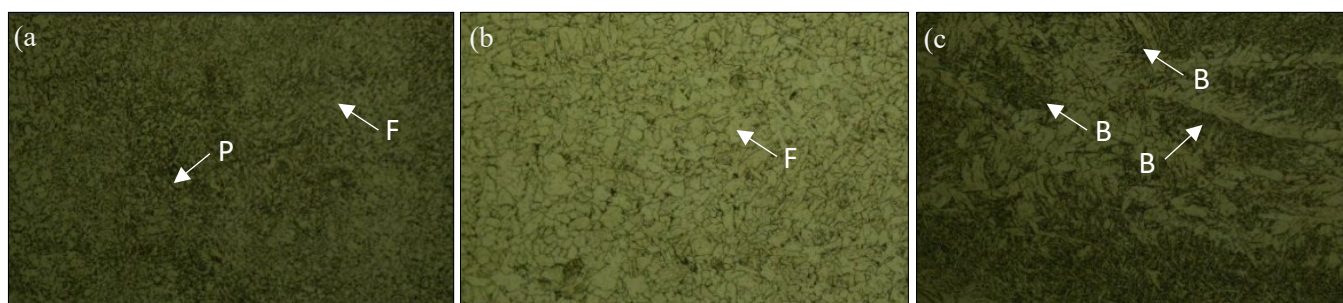


Fig 2: Macrographs of microstructural formation in different zones of the thin wall; (a) lower zone; (b) middle zone; (c) upper zone adapted from the research journal by Liberini et al [16]

Fig 3 depicts the micrography findings extracted from the research journal of Liberini et al. [16]. The middle zone (Fig 3b) of the thin wall has a microstructural formation of evenly spaced pure ferrite (F) grains, where the grain size is coarser than the microstructure formed in the lower zone of the thin wall. This is caused by the higher thermal shock experienced by the lower zone of the thin wall compared to the middle zone. The middle zone of the thin wall has a lower cooling rate compared to the upper zone. However, when compared to the lower zone of the thin wall, the thermal gradient is lower in the middle zone. The lower zone (Fig 3a) of the thin wall has a slower cooling rate compared to the upper zone which explains the ferrite (F) formation, whereas the thermal shock experienced by the cold base metal explains the presence of pearlite (P) microstructure. The upper zone (Fig 3c) of the thin wall experiences a higher level

of thermal shock, which explains the lamellar bainitic (B) microstructural formation with laths aggregate consisting of both the ferritic (F) and cementite (C) microstructure.

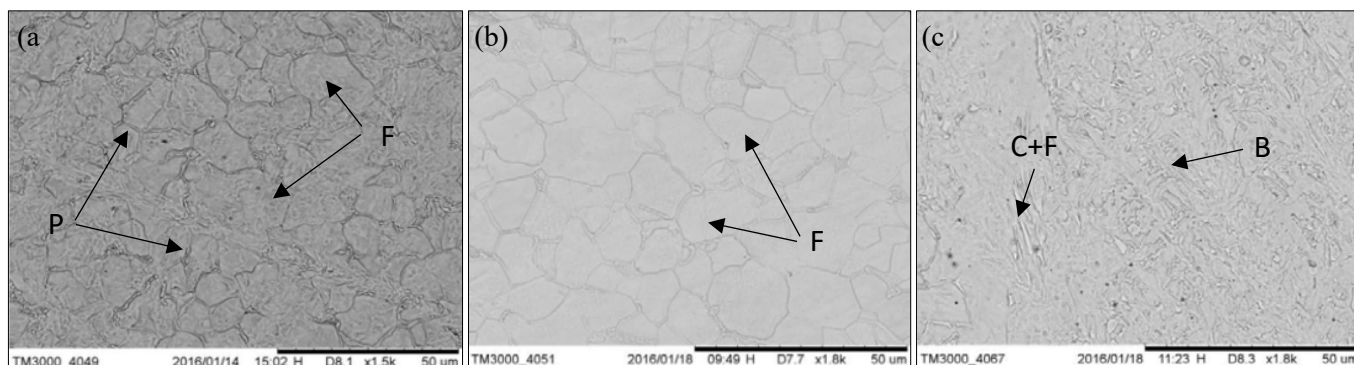


Fig 3: Micrographs of microstructural formation in different zones of the thin wall; (a) lower zone; (b) middle zone; (c) upper zone [16] adapted from the research journal by Liberini et al. [16]

Separate research was conducted by Rafieazad et al. [18] on ER70S-6 low-carbon, low-alloy steel wall manufactured using a GMAW-based additive manufacturing employing an advanced surface tension transfer (STT) method. In their research, it was determined that the microstructure formation changes from a region near the fusion line to the core of the molten metal. In the centre of each molten metal pool, a fine polygonal ferrite (F) microstructural formation made up the primary phase, with a lower volume percentage of a lamellar pearlite (P) phase formed primarily along the grain boundaries of the ferrite microstructure. Separate research done by Haden et al. [19] also found similar microstructural formation in thin walls fabricated using ER70S-6 steel. The microstructure along the molten pool boundaries revealed the formation of acicular ferrite (AF) and bainite (B) near the molten pool boundaries. This microstructure formation occurs as a result of overlapping scanning lines and solidification of deposited molten metal, resulting in distinct thermal histories from the centre of each molten pool to the margins of the next deposited molten pool [20]. A higher cooling rate around the fusion boundaries resulted in the formation of non-equilibrium AF and Bainite phases. Haselhuhn et al. [21] found similar microstructural changes from polygonal ferrite to acicular ferrite from the centre of the molten pool to the boundaries of the molten pool in an ER70S-6 wall produced by the WAAM process due to increased cooling rates during solidification along the fusion line. To quantify the volume fraction of the pearlite phase formed along the ferrite grain boundaries, Rafieazad et al. [18] conducted a detailed image analysis of the microstructure from various locations of the sample using the ImageJ software. From their observation, it was concluded that the feedstock wire (ER70S-6) has a low carbon content in the approximate range of 0.06% to 0.15%, resulting in a volume percentage of the pearlite phase of only $12.54 \pm 0.56\%$ of the total microstructure of their tested sample.

3.2 Vickers Microhardness Evaluation

Rafieazad et al. [18] conducted a Vickers hardness evaluation of the thin wall produced using the GMAW-based WAAM process, which utilizes the ER70S-6 low-carbon low-alloy steel deposited by the advanced surface tension transfer (STT) mode. The microhardness evaluation of their samples was obtained along the as-built wall in a vertical direction, starting from the lower zone of the as-built wall to the upper zone of the as-built wall. A 10mm margin from the top and bottom part of the as-built wall was not accounted for during the microhardness evaluation to eliminate the effects of dilution and the final deposited layers. Their results revealed that the average value of the microhardness of the tested as-built wall was 160 ± 7 HV, and a uniform hardness was distributed along the as-built wall, which is the result of consistent microstructural formation found along the tested area. Along the evenly distributed microhardness value, there was also an error of about ± 7 HV due to the variation of micro-constituents found in the grain boundaries of the molten pool and the centre of the molten pool. The highest microhardness value was 175 ± 2 HV, which is found in regions of the molten pool with an acicular ferrite and bainite (AF + B) microstructural formation. The lowest microhardness value was 150 ± 1 HV, which is found in regions with a coarse polygonal ferrite and pearlite (F+P) microstructural formation found in the heat-affected zone (HAZ). HV for regions with dominant microstructures, including the fine ferrite and pearlite lamellae at the ferrite boundaries, the average microhardness value is 160 ± 2 HV.

In separate research conducted by Dekis et al. [22], the hardness properties of ER70S-6 steel produced by the WAAM process were investigated with a focus on the influence of travel speed on the microstructure and mechanical properties. Their study presents a comprehensive analysis of the microhardness evaluation, tensile strength evaluation, and elongation evaluation of the ER70S-6 steel at different travel speeds of 120, 150, and 180 mm/min, respectively. Their results reveal that at higher travel speeds, particularly at 180 mm/min, there is a significant effect on the microstructural formation due to the reduction in the number of pores and cracks formation. The reduction of said defects leads to notable improvements in the mechanical properties, including yield strength and ultimate tensile strength of their tested sample. The ultimate tensile strength achieves a value of up to 502.3 ± 3.17 MPa at the highest travel speed, which is approximately 93% of the catalogued value for the ER70S-6 steel, which is 540 MPa. Although this represents a significant enhancement, the ultimate tensile strength remains slightly lower than the catalogued value, indicating a mild softening effect. This effect is likely caused by the thermal cycles and rapid cooling associated with higher travel speeds, which can influence the microstructure and hardness of the material. The microhardness evaluation results from their research [22] provided further insight into the performance of the ER70S-6 steel. The variations in hardness are attributed to the differences in cooling rates and grain size induced by the travel speed. Higher travel speeds tend to promote finer microstructures due to rapid solidification, which in turn enhances the hardness of the material.

4. Conclusion

In conclusion, the comprehensive examination of additive manufacturing, specifically focusing on wire arc additive manufacturing (WAAM) and its applications in producing ER70S-6 steel components, underscores the transformative potential of this technology in modern manufacturing. Additive manufacturing's ability to build complex geometries layer-by-layer revolutionizes traditional manufacturing processes by enabling unparalleled customization and reducing material waste, thereby aligning with sustainable practices. This efficiency in design and material use is particularly advantageous in industries such as aerospace, automotive, and medical devices, where precision and reliability are paramount. The studies conducted by Liberini et al. [16] and Rafieazad et al. [18] provide significant insights into the microstructural formation and mechanical properties of ER70S-6 steel produced by WAAM. Liberini et al. [16] highlight the heterogeneous microstructures formed due to the distinct thermal cycles in the WAAM process, including bainitic lamellar structures in the upper zone and equiaxed ferrite grains with thin pearlite strips in the middle and lower zones. These findings illustrate the impact of thermal gradients and heat accumulation on the final microstructure, which is critical for optimizing mechanical properties. Rafieazad et al. [18] further emphasize the influence of cooling rates and thermal shocks on the formation of various microstructures, such as acicular ferrite and bainite near the molten pool boundaries. Their detailed image analysis and Vickers hardness evaluation reveal that the low carbon content in ER70S-6 steel results in a relatively low volume percentage of the pearlite phase, which, along with the uniform distribution of microhardness, reflects the consistent quality of the WAAM-produced material. The highest microhardness values are associated with regions containing acicular ferrite and bainite, while the lowest values are found in coarse polygonal ferrite and pearlite regions, highlighting the relationship between microstructure and hardness. Additionally, Dekis et al. [22] study on the effect of travel speed on the mechanical properties of WAAM-produced ER70S-6 steel provides valuable insights. Higher travel speeds, particularly at 180 mm/min, significantly enhance mechanical properties by reducing defects such as pores and cracks. The resulting finer microstructures due to rapid solidification improve the material's hardness and tensile strength, although a mild softening effect is noted compared to the catalogued values. Overall, the diverse microstructural formations and mechanical properties observed in these studies underscore the importance of optimizing process parameters in WAAM. By fine-tuning variables such as travel speed and heat input, manufacturers can enhance the performance and reliability of WAAM-fabricated components. Continued research and development in this field will further expand the capabilities and applications of additive manufacturing, solidifying its role as a cornerstone of modern manufacturing technology.

Acknowledgement

This work was supported by a grant from Universiti Malaysia Kelantan, 17600 Jeli, Kelantan [grant number R/MTCH/A1300/00896A/003/2021/00972]. All sponsorships and support are gratefully acknowledged.

References

- [1] Zhou L, Miller J, Vezza J, Mayster M, Raffay M, Justice Q, Al Tamimi Z, Hansotte G, Sunkara L D, & Bernat J. Additive Manufacturing: A Comprehensive Review. *Sensors*, 2024;24(9):2668.
- [2] Additive manufacturing explained | MIT Sloan. (2017, December 7). MIT Sloan.
- [3] Ponis S, Aretoulaki E, Maroutas T N, Plakas G, & Dimogiorgi K. A Systematic Literature Review on Additive Manufacturing in the Context of Circular Economy. *Sustainability*, 2021;13(11):6007.
- [4] Amfg, & Amfg. (2020, March 16). An Introduction to Wire Arc Additive Manufacturing [2020 Update] - AMFG. AMFG - Tomorrow's Manufacturing Today.
- [5] RAMLAB. (2023, November 22). WAAM explained - Wire Arc Additive Manufacturing - RAMLAB.
- [6] McAndrew A R, Rosales M A, Colegrove P A, Hönnige J R, Ho A, Fayolle R, Eyitayo K, Stan I, Sukringpang P, Crochemore A, & Pinter Z. Interpass rolling of Ti-6Al-4V wire + arc additively manufactured features for microstructural refinement. *Addit Manuf*, 2018;21:340-349.
- [7] Jafari D, Vaneker T H, & Gibson I. Wire and arc additive manufacturing: Opportunities and challenges to control the quality and accuracy of manufactured parts. *Mater Des*, 2021;202:109471.
- [8] Saleh B, Fathi R, Tian Y, Radhika N, Jiang J, & Ma A. Fundamentals and advances of wire arc additive manufacturing: materials, process parameters, potential applications, and future trends. *Arch Civ Mech Eng*, 2023;23(2).
- [9] Chen X, Li J, Cheng X, He B, Wang H, & Huang Z. Microstructure and mechanical properties of the austenitic stainless steel 316L fabricated by gas metal arc additive manufacturing. *Mater Sci Eng A*, 2017;703:567-577.
- [10] Xiong J, Li Y, Li R, & Yin Z. Influences of process parameters on surface roughness of multi-layer single-pass thin-walled parts in GMAW-based additive manufacturing. *J Mater Process Technol*, 2017;252:128-136.
- [11] Yang D, He C, & Zhang G. Forming characteristics of thin-wall steel parts by double electrode GMAW based additive manufacturing. *J Mater Process Technol*, 2015;227:153-160.
- [12] Li X, Ma X, Subramanian S, Shang C, & Misra R. Influence of prior austenite grain size on martensite-austenite constituent and toughness in the heat affected zone of 700MPa high strength linepipe steel. *Mater Sci Eng A*, 2014;616:141-147.
- [13] Davis C L, & King J E. Cleavage initiation in the intercritically reheated coarse-grained heat-affected zone: Part I. Fractographic evidence. *Metall Mater Trans A*, 1994;25(3):563-573.
- [14] Zhang C, Song X, Lu P, & Hu X. Effect of microstructure on mechanical properties in weld-repaired high strength low alloy steel. *Mater Des*, 2011;36:233-242.
- [15] Sridharan N, Noakes M W, Nycz A, Love L J, Dehoff R, & Babu S. On the toughness scatter in low alloy C-Mn steel samples fabricated using wire arc additive manufacturing. *Mater Sci Eng A*, 2017;713:18-27.
- [16] Liberini M, Astarita A, Campatelli G, Scippa A, Montevecchi F, Venturini G, Durante M, Boccarusso L, Minutolo F M C, & Squillace A. Selection of optimal process parameters for wire arc additive manufacturing. *Procedia CIRP*, 2017;62:470-474.
- [17] Ding D, Pan Z, Cuiuri D, & Li H. A multi-bead overlapping model for robotic wire and arc additive manufacturing (WAAM). *Robot Comput Integr Manuf*, 2014;31:101-110.
- [18] Rafieezad M, Ghaffari M, Nemani A V, & Nasiri A. Microstructural evolution and mechanical properties of a low-carbon low-alloy steel produced by wire arc additive manufacturing. *Int J Adv Manuf Technol*, 2019;105(5-6):2121-2134.
- [19] Haden C, Zeng G, Carter F, Ruhl C, Krick B, & Harlow D. Wire and arc additive manufactured steel: Tensile and wear properties. *Addit Manuf*, 2017;16:115-123.
- [20] Colegrove P A, Coules H E, Fairman J, Martina F, Kashoob T, Mamash H, & Cozzolino L D. Microstructure and residual stress improvement in wire and arc additively manufactured parts through high-pressure rolling. *J Mater Process Technol*, 2013;213(10):1782-1791.
- [21] Haselhuhn A S, Wijnen B, Anzalone G C, Sanders P G, & Pearce J M. In situ formation of substrate release mechanisms for gas metal arc weld metal 3-D printing. *J Mater Process Technol*, 2015;226:50-59.
- [22] Dekis M, Tawfik M, Egiza M, & Dewidar M. Unveiling the Characteristics of ER70S-6 low Carbon Steel Alloy Produced by wire arc Additive Manufacturing at Different Travel Speeds. *Met Mater Int*, 2024.